

Figure 42. Two small time series $\{X_{1,t}\}$ and $\{X_{2,t}\}$, each with $N = 16$ values. The left-hand plot shows $X_{1,t}$ versus t for $t = 0, \dots, 15$ as black dots, while the right-hand plot shows $X_{2,t}$. The two series differ only at the $t = 13$ th value, for which $X_{2,13} = -X_{1,13}$. For the record, the 16 values for $\{X_{1,t}\}$ are 0.2, -0.4, -0.6, -0.5, -0.8, -0.4, -0.9, 0.0, -0.2, 0.1, -0.1, 0.1, 0.7, 0.9, 0.0 and 0.3.

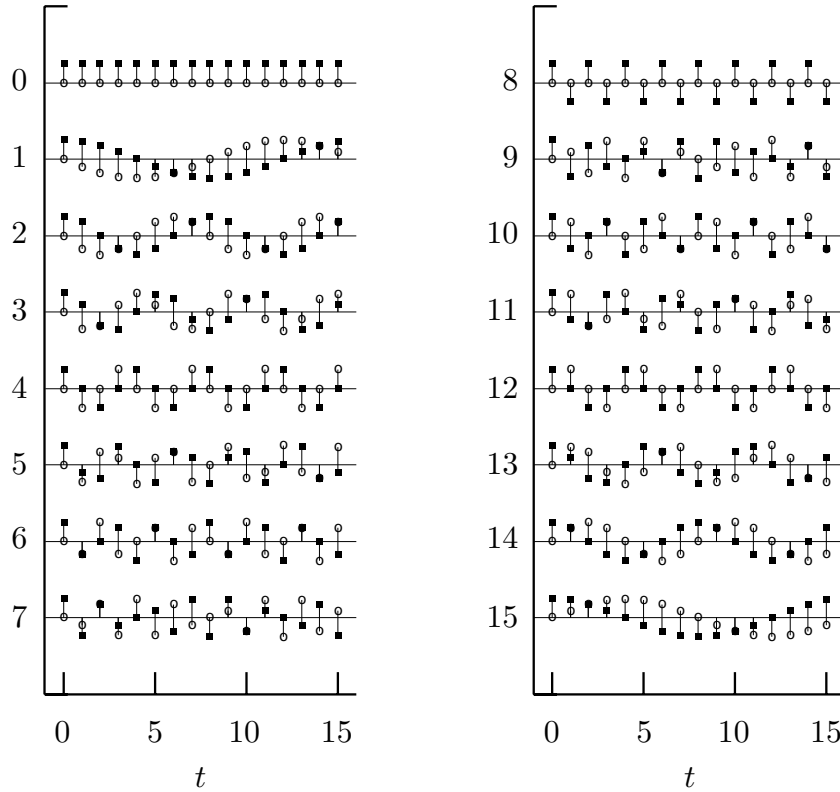


Figure 47. Row vectors $\mathcal{F}_{k\bullet}^H$ for the orthonormal discrete Fourier transform matrix \mathcal{F} for $N = 16$ and $k = 0$ to 7 (top to bottom on left-hand plot) and $k = 8$ to 15 (right-hand plot). Most of the elements of \mathcal{F} are complex-valued, so the real and imaginary components are represented, respectively, by solid squares and open circles. Note that the elements of $\mathcal{F}_{0\bullet}^H$ and $\mathcal{F}_{8\bullet}^H$ are real-valued and that, e.g., $\mathcal{F}_{15\bullet}^H = (\mathcal{F}_{1\bullet}^H)^*$.

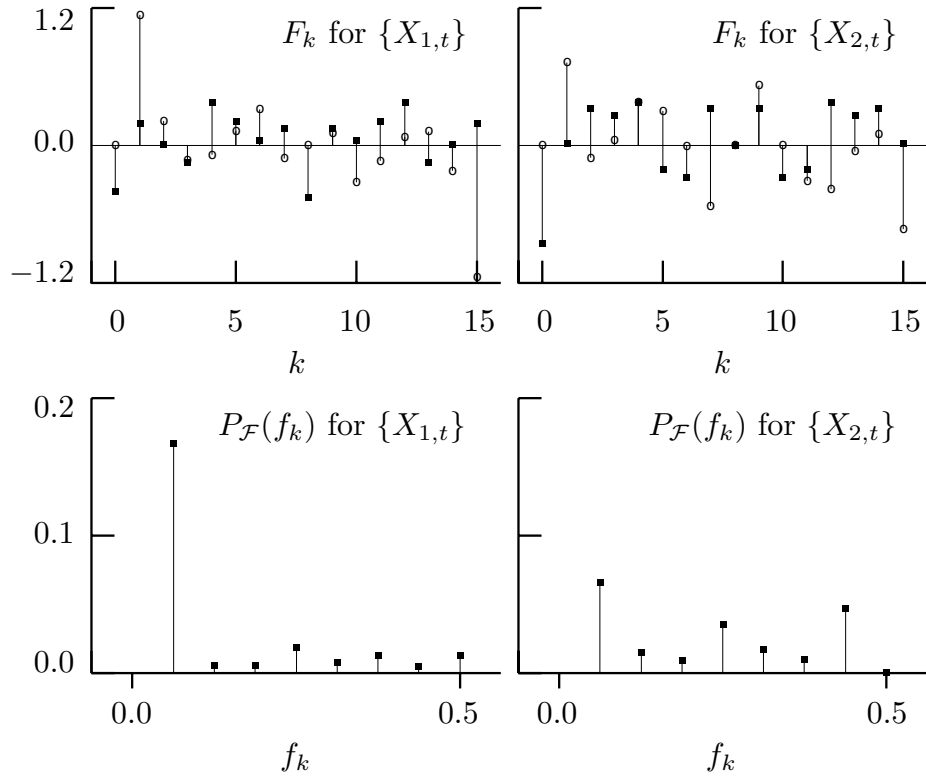


Figure 49. Orthonormal discrete Fourier transforms for the time series in Figure 42. The ODFTs \mathbf{F} for $\{X_{1,t}\}$ and $\{X_{2,t}\}$ are plotted in the top row. The real and imaginary components of the ODFTs are represented by, respectively, solid squares and open circles. The discrete empirical power spectra corresponding to these ODFTs are shown in the bottom row.

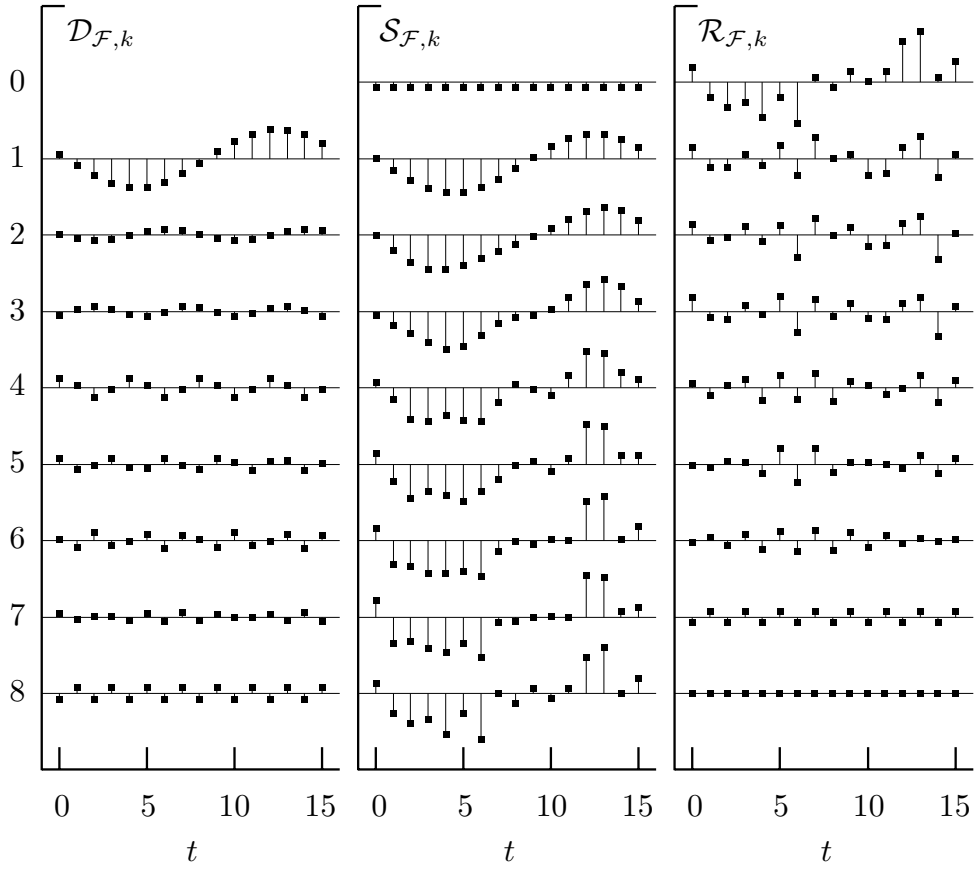


Figure 50. Fourier details $\mathcal{D}_{\mathcal{F},k}$, smooths $\mathcal{S}_{\mathcal{F},k}$ and roughs $\mathcal{R}_{\mathcal{F},k}$ for $\{X_{1,t}\}$ (left-hand plot of Figure 42) for $k = 0, \dots, 8$ (top to bottom).

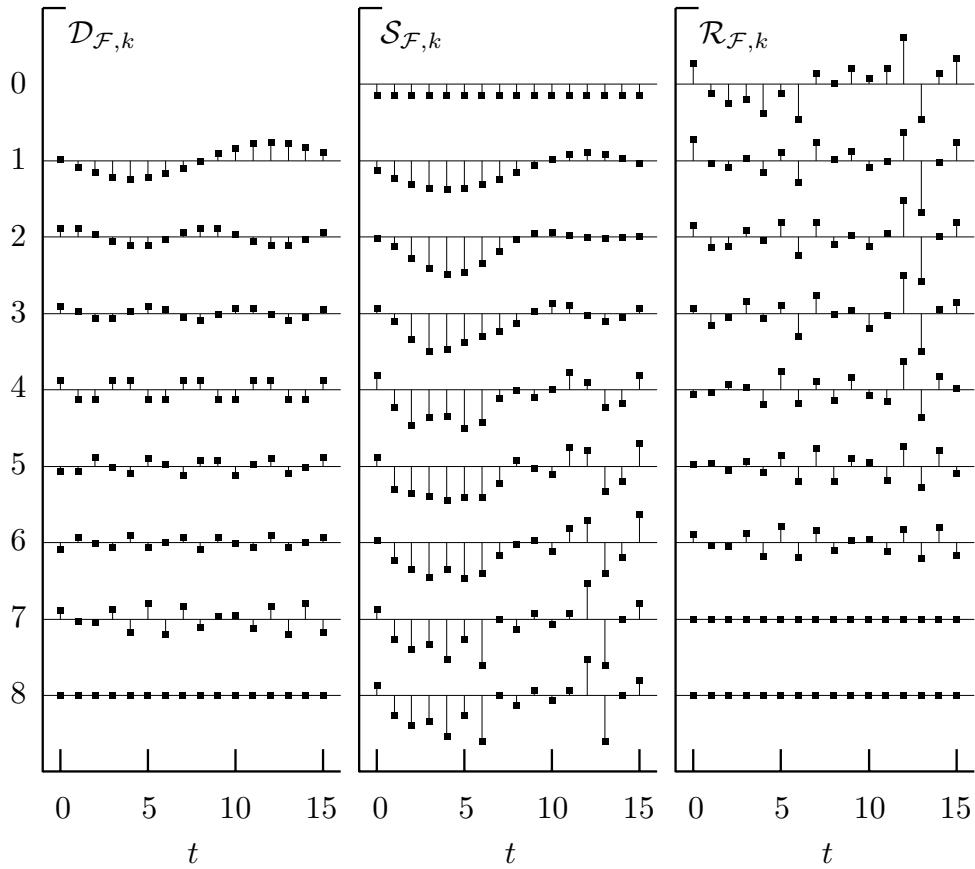


Figure 51. Fourier details $\mathcal{D}_{\mathcal{F},k}$, smooths $\mathcal{S}_{\mathcal{F},k}$ and roughs $\mathcal{R}_{\mathcal{F},k}$ for $\{X_{2,t}\}$ (right-hand plot of Figure 42) for $k = 0, \dots, 8$ (top to bottom).